

A REVIEW OF STOCHASTIC DESCRIPTION OF THE TURBULENCE EFFECT ON BUBBLE-PARTICLE INTERACTIONS IN FLOTATION

Anh V. Nguyen^{1*}, Duc-Anh An-Vo², Thanh Tran-Cong² and Geoffrey M. Evans³

¹School of Chemical Engineering, The University of Queensland, Brisbane, QLD 4072, Australia

²Computational Engineering and Science Research Centre, The University of Southern Queensland, Toowoomba, QLD 4350, Australia

³School of Engineering, The University of Newcastle, Callaghan, NSW 2308, Australia

*Corresponding author: email anh.nguyen@eng.uq.edu.au; Telephone +61 7 336 53665

ABSTRACT

Flotation in mechanically agitated cells has been the workhorse of the mining industry, but our quantitative understanding of the effect of microturbulence generated by agitation on flotation is still very limited. This paper aims to review the literature on quantifying the microturbulence effects on bubble-particle interactions in flotation. The particular focus is on the stochastic description of bubble-particle interactions in the turbulent flow which is a random field. We briefly review the stochastic description of microturbulence and motions of particles of micrometre sizes and bubbles of millimetre sizes in the isotropic turbulence of mechanical flotation cells. The key starting point is the generic equation of motion, which can be decomposed into the mean turbulent variables and fluctuating turbulent variables. The turbulent flow of the carrying liquid is characterised using isotropic turbulence theory. The next focus is on reviewing bubble-particle turbulent collision and detachment interactions. Bubble-particle turbulent collision is poorly quantified; no quantitative models of the bubble-particle turbulent collision efficiency relevant for flotation are available. Current theories on bubble-particle turbulent detachment face some deficiencies. In assessing the microturbulence effect on bubble-particle detachment, the majority of studies only consider the particle acceleration in the centrifugal direction but ignore the transverse acceleration of particles, which is due to turbulent shear flow. Critically, contact angle required in quantifying the detachment is not constant, single-valued as considered in the theories, but can vary from receding to advancing value during the relaxation of the triple contact line on the particle surface. The latest experiments show that multiple-valued contact angle can significantly affect stability and detachment of floating particles. Finally, quantifying the microturbulence effect on flotation requires further research.

Keywords: collision, detachment, turbulence, mixing, minerals

1. INTRODUCTION

Froth flotation is an industrially important process which has been used for more than a 100 years to recover valuable minerals from the Earth's crust (Lynch et al., 2010). It uses the differences in the affinity (hydrophobicity) of solid particles to air bubbles rather than water. Froth flotation is usually preceded by crushing and grinding the ore to liberate the valuable mineral particles from the rock. The slurry is mixed with flotation reagents to control the difference in hydrophobicity between the wanted and unwanted particles. Air is then introduced into the slurry and dispersed into fine bubbles of 1-3 mm in diameter by turbulence generated by agitation. The air bubbles collect the hydrophobic (wanted) mineral particles and rise to the slurry surface, where they form a froth layer, overflowing the lip of the cell into the concentrate launder. This very simplistic description of the widely-used flotation process in the mineral industry highlights the important role of turbulence in flotation. Indeed, the modelling of the flotation macro- and micro-processes requires the application of the statistical turbulence theory as discussed by many flotation scientists, including Professor Schubert et al. (Schubert and Bischofberger, 1978). The significant effect of turbulence on the flotation macro-process is usually considered via the turbulent transport phenomena, including suspension and transport of solid particles to avoid the sanding problem occurring at the bottom of the cells and turbulent entrainment of solid particles from the pulp phase into the froth phase (Guerra and Schubert, 1997). Turbulence can significantly affect the following flotation micro-processes (Schubert and Bischofberger, 1998; Nguyen and Schulze, 2004):

- Turbulent dispersion of air into fine bubbles
- Turbulent bubble-particle collision, and
- Turbulent bubble-particle detachment.

The turbulent transport phenomena of flotation are controlled by macro-turbulence which is defined by the size and geometry of turbulence-generating devices and is not considered in this review. The flotation micro-processes are significantly controlled by micro-turbulence, which is universal and does not depend on the size and geometry of turbulence-generating devices. This review focuses on the literature which describes the effect of microturbulence on flotation.

2. ISOTROPIC TURBULENCE

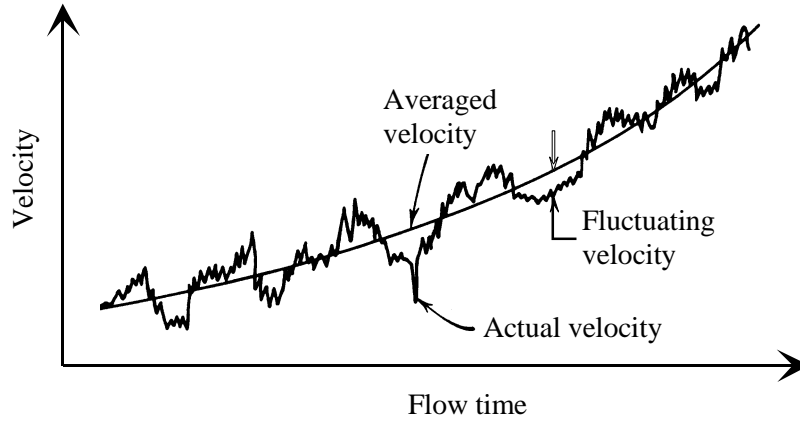


Figure 1. Schematic of the actual, time-averaged and fluctuating velocities of turbulent flow as a function of time (Nguyen and Schulze, 2004).

Turbulent flow is characterized by random fluctuations in the flow variables as illustrated for the turbulent velocity of fluid particles in Figure 1. Therefore, turbulent flows require statistical techniques for their analysis, and the theory of turbulent flow is statistical in nature. Both the mean (time-averaged) and fluctuating turbulent variables are relevant for analysing flotation micro-processes which are controlled by microturbulence. The flow velocity, stress and pressure (ϕ) are decomposed into the mean ($\bar{\phi}$) and fluctuating (ϕ') components by $\phi = \bar{\phi} + \phi'$. Substituting these variables into the instantaneous continuity and Navier-Stokes equations and applying time averaging yield the Reynolds-averaged Navier-Stokes equations for the mass and momentum conservations which are useful for further analysis. For instance, the statistical turbulence theory of Kolmogorov (Kolmogorov, 1941) shows that microturbulence (i.e., turbulence of the small eddies in the universal equilibrium range as illustrated in figure 2) depends solely on the turbulent kinetic energy dissipation rate, ε , and the kinematic viscosity, ν , as follows:

$$\lambda_K = (\nu^3 / \varepsilon)^{1/4} \quad (1)$$

$$W_K = (\varepsilon \nu)^{1/4} \quad (2)$$

Dimensional analysis shows that the size, λ , and velocity, W_λ , of turbulent eddies in the equilibrium range is correlated by $W_\lambda = (\lambda \varepsilon)^{1/3}$. The Reynolds number of the turbulent eddies, $Re_\lambda \equiv \lambda W_\lambda / \nu$, of the Kolmogorov scales is equal to 1. For large eddies, Re_λ is large, and dissipation by viscous forces is unimportant. Re_λ decreases with decreasing the eddy scale. At a critical scale, the inertial forces of turbulent eddies are balanced by the viscous forces, which starts affecting the motion of turbulent

eddies. At the critical scale, $Re_\lambda = 1$ as per the Kolmogorov theory. The typical range of microturbulence is shown in Table 1.

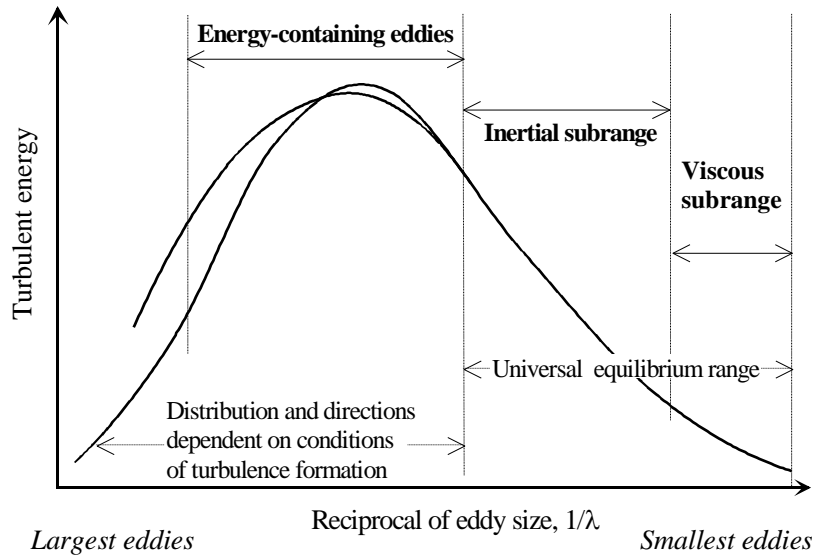


Figure 2. The spectrum of the turbulent energy versus the reciprocal of turbulent eddy sizes. The largest eddies depend on the geometry of the turbulence-generating systems. The medium-size eddies make the main contribution to the kinetic energy. The small eddies are isotropic, independent of the conditions of formation, as described by the universal equilibrium range. The eddy Reynolds number of the smallest eddies at the bottom of the eddy spectrum is equal to 1 (Nguyen and Schulze, 2004).

Table 1. Scales of the smallest laminar and turbulent eddies in water as a function of the energy dissipation rate ε ($\nu = 10^{-6} \text{ m}^2/\text{s}$).

Dissipation rate ε [W/kg]	Scale of the smallest	
	Laminar eddies $\lambda = (4 - 6) \lambda_K$ [μm]	turbulent eddies $\lambda = (10 - 15) \lambda_K$ [μm]
1	130 – 190	320 – 470
10	70 – 110	180 – 270
100	40 – 60	100 – 175

The fluctuating turbulent velocities $w' = w - \bar{w}$ cannot be used to characterize microturbulence since they are conditioned by the large turbulent eddies. Microturbulence can be characterised by the second statistical moment of the velocity increment, $D(r)$ (Kolmogorov, 1941). It is defined by the variance of the fluctuating velocities between close points at distance r as follows:

$$D(r) \equiv \overline{[W'(\mathbf{x}+\mathbf{r},t) - W'(\mathbf{x},t)]^2} \quad (3)$$

where \mathbf{x} is the position vector and $r = |\mathbf{r}|$. $D(r)$ is also known as the structure function of the random scalar field $W(\mathbf{r})$. Because velocity is a vector and can be resolved into the random scalars in the appropriate coordinates, both the longitudinal (D_{ll}) and transverse (D_{nn}) structure functions are obtained by the projections to vector \mathbf{r} and its perpendicular direction. D_{ll} and D_{nn} are linked by the following equation derived from the mass conservation (continuity) equation:

$$D_{nn}(r) = D_{ll}(r) + \frac{r}{2} \frac{dD_{ll}}{dr} \quad (4)$$

It is, therefore, sufficient to consider the structure function in the longitudinal direction, which is customarily described by its square root as follows: $\Delta W \equiv \sqrt{D_{ll}}$.

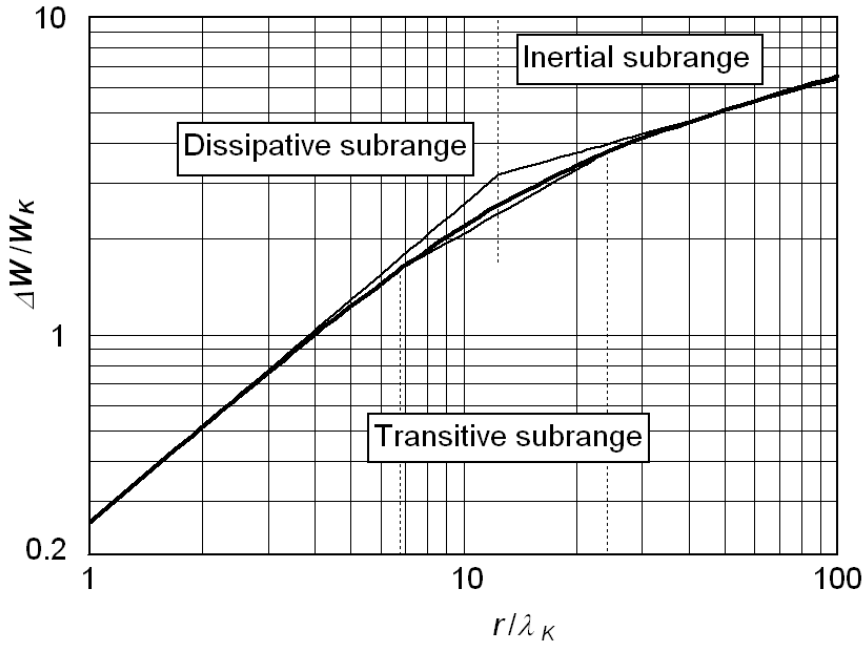


Figure 3. Root-mean-square of the fluctuating velocities of microturbulence in the longitudinal direction between two points separated by a distance r . Eq. (8) is described by the thick line. The thin lines describe the appropriate subranges.

For the smallest eddies $r \sim \lambda_K$, the asymptotic analysis of the Kolmogorov theory gives

$$\Delta W(r) = \left(\frac{\varepsilon}{15\nu} \right)^{1/2} r \quad (5)$$

For large eddies, $\lambda_K \ll r \ll \Lambda$ (macro-turbulence), we have:

$$\Delta W(r) = \sqrt{C}(\varepsilon r)^{1/3} \quad (6)$$

where $C = 2$ is a numerical constant that is universal in the Kolmogorov theory. For the whole range of microturbulence, we can expect the following expression:

$$\Delta W = W_K f(r/\lambda_K) \quad (7)$$

where f is an interpolating function, connecting the two asymptotic expressions described by Eqs. (5) and (6). The asymptotic analysis (Batchelor, 1982) gives the following interpolating function valid in the whole universal equilibrium range (Figure 3):

$$f(x) = \frac{x/\sqrt{15}}{\left[1 + (15C)^{-3/2} x^2\right]^{1/3}} \quad (8)$$

Microturbulence is often divided into the dissipative and inertial subranges (Figure 3). The **dissipative** subrange is used for $r/\lambda_K \leq 5$ to 10. The root-mean-square of fluctuating velocities in this subrange is described by Eq. (5). Eddies in this subrange are laminar. The maximal laminar shear stress in this subrange is given by

$$\tau_{\max} = 0.26\delta\sqrt{\varepsilon\nu} \quad (9)$$

At $0.06\lambda \geq r/\lambda_K \geq 15$ to 20 the inertial transfer of energy from large eddies is the dominant factor, so this is called the **inertial** subrange. The root-mean-square of the difference in the turbulent velocities between sufficiently near points separated by a distance r in this subrange is approximated by Eq. (6) with $C = \sqrt{2}$. Eddies of these scales are turbulent in themselves. The fluctuation of the normal stresses in this subrange is dominant and strongly controls a number of physical processes occurring in the liquid, including the air dispersion and the stability of bubble-particle aggregates in flotation. The root mean square of turbulent pressures (or “dynamic thrust”) in the inertial subrange is determined by Eq. (12).

As some microturbulence processes occur in the range $r/\lambda_K = 5$ to 30, Schubert et al. (Schubert et al., 1990) introduced a **transitive** subrange between the dissipative and inertial subranges. The square root of the velocity variance in this transitive subrange is described as follows:

$$\Delta W = 0.45\varepsilon^{5/12}\nu^{-1/4}r^{2/3} \quad (10)$$

This transitive subrange is valid for $5\lambda_K \leq r \leq 29\lambda_K$.

A common feature of turbulent flows in flotation is the small size of particles and bubbles in comparison with the dimension of the turbulence macroscale. The small eddies are determined by the dissipation of local turbulent energy and the liquid kinematic viscosity, and are within the range of 3 to 4 times of the Kolmogorov microscale. In flotation, they are within the range of 30 to 50 μm . Fine solid particles of the sizes within the range up to $10\lambda_K$ are influenced mainly by laminar eddies in the dissipative subrange. Air bubbles of sizes larger than $10\lambda_K$ are influenced by the inertial eddies.

The pressure and acceleration of turbulent flows are also critical to bubble-particle interactions. Similar to the spatial correlations between turbulent velocities, the turbulent pressure fluctuation can be characterised by the spatial structure function which is defined by $D_{pp}(r) \equiv \overline{[P'(\mathbf{x}+\mathbf{r},t) - P'(\mathbf{x},t)]^2}$. The root mean square of the pressures is often used, giving $\Delta P(r) = \sqrt{D_{pp}(r)}$. It can be described in terms of ΔW expressed by Eq. (7) or its universal function $f(x)$ as follows (Batchelor, 1982):

$$\Delta P(r) = \delta W_K^2 \sqrt{\left(\frac{r}{\lambda_K}\right)^2 \int_{r/\lambda_K}^{\infty} \frac{1}{x} \left(\frac{df^2}{dx}\right)^2 dx + \int_0^{r/\lambda_K} x \left(\frac{df^2}{dx}\right)^2 dx} \quad (11)$$

Upon inserting Eq. (8) for f , Eq. (11) can be numerically integrated. The result of the integration is shown in Figure 4. For large eddies, $f = \sqrt{C}x^{1/3}$ as per Eq. (7) or (8), and Eq. (11) gives

$$\Delta P(r) = \delta C(\varepsilon r)^{2/3} = \delta(\Delta W)^2 \quad (12)$$

Equation (12) is the well-known prediction for spatial pressure change in the inertial subrange ($\lambda_K \ll r \ll A$), which is widely used in predicting the breakage of air bubbles.

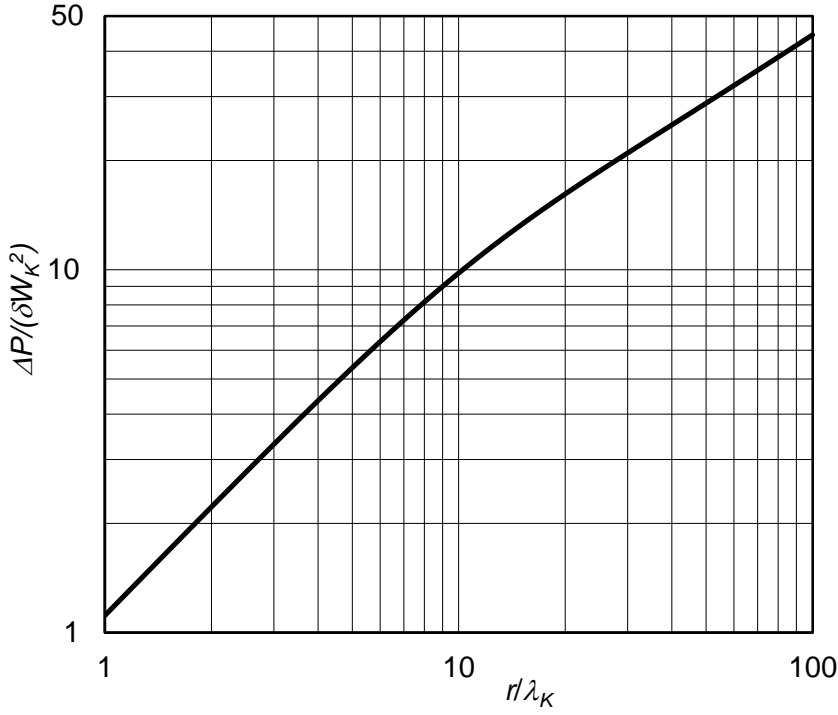


Figure 4. Root-mean-square of the fluctuating pressures of microturbulence between two points separated by a distance r .

The Kolmogorov method of microturbulence analysis can be used to analyse the fluctuation of turbulent acceleration. The period of oscillation of an eddy λ is equal to $T_\lambda \propto \lambda / W_\lambda = \varepsilon^{2/3} \lambda^{-1/3}$. The eddy acceleration, a_λ , follows the proportionality: $a_\lambda \equiv dW_\lambda / dT_\lambda \propto W_\lambda / T_\lambda \propto \varepsilon^{2/3} \lambda^{-1/3}$. The eddy acceleration has two components, as described by the Navier-Stokes equations, the potential acceleration component produced by pressure fluctuation and the solenoidal component produced by viscous forces. Therefore, the spatial correlation of the acceleration field is a tensor which can be described as follows: $\overline{a(\mathbf{x} + \mathbf{r}, t) a(\mathbf{x}, t)} = [B_{ll}(r) - B_{mm}(r)] r_i r_j / r^2 + B_{mm}(r) \delta_{ij}$, where r_i and r_j are the moduli of position vectors, δ_{ij} is the Kronecker delta, and $B_{ll}(r)$ and $B_{mm}(r)$ are the longitudinal and transverse correlation functions of the acceleration field. These correlation functions can be derived from the Navier-Stokes equations (Batchelor, 1982) and yield, for the inertial subrange, where viscous contributions are negligible:

$$B_{ll}(r) = \sqrt{\overline{a_l(\mathbf{x} + \mathbf{r}, t) a_l(\mathbf{x}, t)}} = \frac{1}{2\delta^2} \frac{d^2 D_{pp}(r)}{dr^2} = \frac{8}{9} \frac{\varepsilon^{4/3}}{r^{2/3}} \quad (13)$$

$$B_{mm}(r) = \sqrt{\overline{a_n(\mathbf{x} + \mathbf{r}, t) a_n(\mathbf{x}, t)}} = \frac{1}{2\delta^2 r} \frac{dD_{pp}(r)}{dr} = \frac{8}{3} \frac{\varepsilon^{4/3}}{r^{2/3}} \quad (14)$$

where $D_{pp}(r) = [\Delta P(r)]^2 = \delta^2 C^2 (\varepsilon r)^{4/3} = 4\delta^2 (\varepsilon r)^{4/3}$. The magnitude of the spatial correlation of eddy acceleration, often referred to as the mean “machine acceleration”, can be determined by:

$b_m = \sqrt{B_{ll}(r) + B_{mm}(r)}$, which gives

$$b_m(r) = 1.9 \frac{\varepsilon^{2/3}}{r^{1/3}} \quad (15)$$

The machine acceleration was used in quantifying bubble-particle detachment (Schulze, 1982).

One of the most important parameters determining the turbulent detachment is the rate of energy dissipation. Unfortunately, a numerical value of this parameter is not always available, and a mean dissipation rate is often used. The mean rate is defined as the input power per unit mass of liquid. It is rather a rough estimation for flotation because of the spatial distribution of the actual dissipation in flotation cells. In the impeller-stator region the gradient of the dissipation rate of turbulent energy is the highest. The maximum value of the local dissipation in the impeller region of industrial flotation cells can be higher than the mean value by a factor up to 30. In this region the total power input dissipates, and the dispersion of air into bubbles and the bubble-particle interaction actively occur. The mean turbulent energy dissipation rate obtained by averaging over the total cell volume can be incorrectly used for the modelling of bubble-particle interactions and other micro-processes in flotation. A good estimation should be based on the input power and the volume of the impeller region, where the turbulent bubble-particle interactions take place.

3. MOTION OF PARTICLES AND BUBBLES IN TURBULENT FLOWS AND THEIR INTERACTIONS

Bubble-particle interactions in flotation can be quantified if their motions in the flotation cell are known. Regrettably, we almost always know very little about the exact motions of air bubbles and solid particles in flotation, especially in the turbulent flows of flotation. Consequently, a number of approximate approaches have been applied and useful information has been obtained. A popular approach is to adopt the extensions of the Basset-Boussinesq-Oseen (BBO) equation for the particulate motions in non-stationary fluid (Nguyen and Schulze, 2004). The BBO equation includes steady and unsteady drag, gravitational and inertial forces. For fine particles typically encountered in flotation the extended BBO equation can be described as follows (Nguyen and Schulze, 2004):

$$m_p \frac{d\mathbf{V}}{dt} = m_p \frac{\delta}{\rho_p} \frac{D\mathbf{W}}{Dt} - m_p \frac{\delta}{\rho_p} \frac{1}{2} \left\{ \frac{d\mathbf{V}}{dt} - \frac{d\mathbf{W}}{dt} \right\} - 6\pi\mu R_p (\mathbf{V} - \mathbf{W}) + m_p \left(1 - \frac{\delta}{\rho_p} \right) \mathbf{g} \quad (16)$$

where $D(\dots)/Dt = \partial(\dots)/\partial t + \mathbf{W} \cdot \text{grad}(\dots)$ and $d(\dots)/dt = \partial(\dots)/\partial t + \mathbf{V} \cdot \text{grad}(\dots)$ describe the derivatives following the liquid element and the moving solid particle, respectively. Here, the history Basset term of the dynamic resistance is neglected. Equation (16) is applied to very small particles that ideally satisfy Stokes Law. Empirically, it can be used with particles with a diameter up to 60 μm . For coarse particles, corrections are needed but the most important extension is the correction to the Stokes resistance by multiplying the third term on the right-hand side of Eq. (16) by a factor of $f_d = 1 + 0.169Re^{2/3}$ which is valid for $0 \leq Re < 700$ (Nguyen and Schulze, 2004). Alternatively, the factor of the Oseen correction can be used but is only valid for very small Reynolds number. These two correction factors can permit analytical solutions of the particle motion equation. The Reynolds number is calculated using the local slip velocity.

The description of the motion of air bubbles in flotation is more complicated than that of solid particles. The bubble motion is influenced by the bubble size and shape, physical properties of the medium, and physicochemical properties of the gas-liquid interface (Nguyen and Schulze, 2004). The shape that the bubbles assume during their motion is, in turn, a complex function of the hydrodynamic, viscous and interfacial forces exerted on the bubbles. The liquid drag force on small bubbles may be equal to that on solid particles. The bubble surface may become mobile, and in contrast to that for solid particles, there are non-vanishing tangential velocities at the gas-liquid interface. The gas circulation inside a bubble can also reduce the drag on it. Importantly, flotation reagents and surface contaminants can have a significant effect on the bubble hydrodynamics. They can adsorb onto the bubble surface, retard the bubble mobility and restore the shape of small bubbles to a sphere or spheroid. The drag force on air bubbles rising through a flotation pulp usually follows the drag force on bubbles in grossly contaminated water. Therefore, the following equation can be used to describe the motion of air bubbles in the turbulent flow of flotation:

$$m_b \frac{d\mathbf{U}}{dt} = m_b \frac{\delta}{\rho_b} \frac{D\mathbf{W}}{Dt} - m_b \frac{\delta}{\rho_b} \frac{1}{2} \left\{ \frac{d\mathbf{U}}{dt} - \frac{d\mathbf{W}}{dt} \right\} - 6\pi\mu R_b (\mathbf{U} - \mathbf{W}) f_d + m_b \left(1 - \frac{\delta}{\rho_b} \right) \mathbf{g} \quad (17)$$

where $d(\dots)/dt = \partial(\dots)/\partial t + \mathbf{U} \cdot \text{grad}(\dots)$ describe the derivatives following the moving bubble. Eq. (17) is similar to Eq. (16), except for the correction factor, $f_d = 1 + 0.169Re^{2/3}$, for the drag force which must be included because of the millimetre size of air bubbles used in flotation. Here, the

local bubble Reynolds number is defined as $Re = 2R_b |\mathbf{U} - \mathbf{W}| / \nu$. The history Basset term of the dynamic resistance is also neglected.

Both Eqs. (16) and (17) show that the motions of solid particles and air bubbles are controlled by the gravitational, inertial and liquid flow forces. These forces can have strong effects on bubble-particle interactions, and are usually included in the predictions of bubble-particle interactions. Their effects on bubble-particle interactions in flotation are usually coupled. Therefore, the final effect of these forces on bubble-particle collision, attachment and detachment interactions is difficult to predict by linear combinations of the individual effects. The exact solutions of the motion equations are not always attainable. The mobility of the bubble surface can be introduced into quantifying the bubble-particle interactions through the boundary conditions at the air-water interface applied to the water velocity. As can be seen from Eqs. (16) and (17), both the particle and bubble velocities required for quantifying bubble-particle interactions can be calculated if the water velocity is known. Therefore, the modelling of the bubble-particle interactions is usually preceded by the modelling of the water flow field and then the modelling of the particle and bubble velocities using the BBO equations.

The motion equations for both the solid particles and air bubbles in turbulent flows, described by Eqs. (16) and (17), respectively, are nonlinear and therefore difficult to be solved analytically. Some approximations have been obtained. For example, in the case of fine particles which are entrained in the turbulent water flow, after applying the Reynolds decomposition, Eq. (16) can be transformed to the following equation for the fluctuating variables:

$$\frac{d\mathbf{V}'(t)}{dt} + \frac{1}{T} \mathbf{V}'(t) = \frac{3\delta}{2\rho_p + \delta} \frac{d\mathbf{W}'(t)}{dt} + \frac{1}{T} \mathbf{W}'(t) \quad (18)$$

where the relaxation time, T , of the particle with a “joined mass” is described by

$$T = \frac{2}{9\mu} \left(\rho_p + \frac{1}{2} \delta \right) R_p^2 \quad (19)$$

It is noted that $\bar{V} - \bar{W} = 2(\rho_p - \delta)gR_p^2 / (9\mu)$ is the Stokes velocity for particle settling and is utilised in establishing Eq. (18). Employing the initial condition: $\mathbf{V}'(0) = \mathbf{W}'(0) = 0$, Eq. (18) can be solved to obtain the following prediction for the particle fluctuating velocity:

$$\mathbf{V}'(t) = \frac{3\delta}{2\rho_p + \delta} \mathbf{W}'(t) + \frac{2\rho_p - 2\delta}{2\rho_p + \delta} \frac{1}{T} \int_0^t e^{-\frac{\tau}{T}} \mathbf{W}'(t - \tau) d\tau \quad (20)$$

Equation (20) provides a special relationship between the fluctuating velocities of the water and fine solid particles which are entrained in the water turbulent flow. They are the random variables but can be used for demonstrating the effect of water turbulence on bubble-particle collision interaction.

Particle-bubble interaction underpins the flotation process, and is normally divided into collision, attachment and detachment (Jameson and S. Nam, 1977; King, 2001; Nguyen and Schulze, 2004). Collision is the approach of a particle to encounter a bubble and is governed by the mechanics of the bubbles and particles in the turbulent flow field. The limit of the collision process is determined by the zonal boundary between the long-range hydrodynamic and interfacial force interactions (Nguyen and Schulze, 2004). The inter-surface separation distance at the zonal boundary between a bubble and a particle is of the sub-micrometre order. Once the particle approaches the bubble at a shorter separation distance, the molecular forces are significant, and the attachment process starts. The detachment process is governed by the capillary force, the particle weight and the detaching forces of the turbulent flow. The governing mechanisms of long-range hydrodynamics, surface chemistry, and capillarity are largely independent, and each of them has a significant influence on only one of the three elements of the bubble-particle interaction. Consequently, collision, attachment and detachment can be mathematically treated independently, which significantly simplifies the task of modelling each of the interactions. The following sections focus on the effect of turbulence on the collision and detachment interactions.

4. EFFECT OF TURBULENCE ON BUBBLE-PARTICLE COLLISION INTERACTION

The theories of bubble-particle collision (encounter) interaction can be deterministic or stochastic. These theories aim to predict the collision rate and efficiency. The available theories are based on the assumption that motions of bubbles and particles in flotation are deterministic. Consequently, these theories are evidently not able to describe the collision interactions affected by fluctuating components of turbulence which are not deterministic. The available deterministic theories, however, can be applied to describe the collision interactions controlled by the mean components of turbulent flow which are determined by large (energy-containing) turbulent eddies and turbulence-generating devices.

The bubble-particle collision rate, N_c , is defined as the number of particles colliding with a bubble per unit time, and can be described as follows:

$$N_c = \iint \mathbf{J} \cdot d\mathbf{S}_b = \iint n_p \Delta \mathbf{V} \cdot d\mathbf{S}_b \quad (21)$$

where $\mathbf{J} = n_p \Delta \mathbf{V}$ is the flux of the free (unattached) particles moving relatively to the bubble with a relative velocity $\Delta \mathbf{V}$, n_p the particle number density (concentration), and the surface element vector $d\mathbf{S}_b$ is the vector of the bubble surface normal—defined as one particle radius away from, and pointing towards the bubble surface. Equation (21) can be applied to modelling both the deterministic and stochastic collision interactions in flotation. Utilising the literature involving turbulent gas-particle flows and turbulent coagulation (Williams and Crane, 1983; Kruis and Kusters, 1997), the collision rate is defined by the collision frequency function (or kernel), β , yielding

$$N_e = n_p \beta \quad (22)$$

where β is the number of collisions per unit time and volume.

Collision efficiency, E_c , is defined as the ratio of the real, N_{cr} , to ideal, N_{ci} , collision rates calculated based on Eq. (21) for the particle motions towards the bubble: $E_c = N_{cr} / N_{ci}$. In calculating the ideal collision rate, N_{ci} , the particle motion is considered not to be influenced by the presence of the bubble, yielding (Nguyen and Schulze, 2004)

$$N_{ci} = \pi n_p (R_p + R_b)^2 (V_p + U_b) \quad (23)$$

where V_p and U_b are the terminal velocities of particle settling and bubble rising, respectively. Equation (23) links the bubble-particle interactions with flotation kinetics based on the first principle (Nguyen and Schulze, 2004). In flotation, solid particles are small, and their motion around the bubbles is solenoidal. The particle concentration in Eq. (21) can be taken outside the integral and we obtain the following generic equation for collision efficiency:

$$E_c = \frac{\oint \Delta \mathbf{V} \cdot d\mathbf{S}_b}{\pi (R_p + R_b)^2 (U_p + U_b)} = \frac{\beta}{\pi (R_p + R_b)^2 (U_p + U_b)} \quad (24)$$

where $\beta = \oint \Delta \mathbf{V} \cdot d\mathbf{S}_b$ is obtained by comparing Eqs. (21) and (22) under the solenoidal condition. The calculation of the integral in Eq. (24) is central to developing the theories of bubble-particle collision interaction.

In flotation cells the bubbles rise to the surface whilst the particles settle to the bottom unless they are captured by the bubbles. The process can generally be considered as a counter-

current operation with the collision interaction occurring at the upper part of the bubble surface where the particles approach the bubble. Therefore, the integration in Eq. (24) is limited by the bubble equator. The collision interaction cannot occur at the bubble equator, but is limited by a polar angle, φ_c , (measured from the upper pole of bubble surface) smaller than 90 degrees, leading to $E_c = 2 \int_0^{\varphi_c} (-\mathbf{e}_r \cdot \Delta \mathbf{V}) \sin \varphi d\varphi / (V_p + U_b)$, where \mathbf{e}_r is the unit vector of the bubble surface normal. The deviation of φ_c from 90 degrees is due to a number of reasons, including the fore-and-aft asymmetry of water flow around air bubbles (Dobby and Finch, 1986; Nguyen and Schulze, 2004), centrifugal forces (Dai et al., 1998) and inertial forces (Ralston et al., 1999; Nguyen and Schulze, 2004). The fore-and-aft asymmetry is due to the millimetre size of the air bubbles used in flotation, which have a Reynolds number, Re , usually in the range 1-500. For this intermediate range of Reynolds numbers the nonlinear (viscous) term in the Navier-Stokes equations is important and can cause the water streamlines to become more compressed towards the upper bubble surface than the lower surface. The fore-and-aft asymmetry is more significant for bubbles with an immobile surface than bubbles with a mobile surface. Since the Stokes and potential flows are fore-and-aft symmetric their linear combination does not predict and represent the fore-and-aft asymmetric water flow around air bubbles in flotation realistically and, therefore, the deterministic theories (Yoon and Luttrell, 1989; King, 2001) developed based on the simple linear combination of the Stokes and potential flows are evidently of artefact. These complicated details have led to many simplified deterministic theories. The model developments are covered by a number of reviews (Dai et al., 2000; Phan et al., 2003; Kostoglou et al., 2006; Nguyen, 2011) and are not repeated here. Table 2 shows a summary of the available deterministic models which are helpful for the discussion in this paper.

Table 2. Deterministic models for bubble-particle collision efficiency (Nguyen, 2011)

Author(s)	Collision efficiency, E_c	Notes and symbol definitions
(Sutherland, 1948)	$E_c = 3R$ where $R = R_p / R_b$	Interceptional effect; potential flow. R is the interception number.
(Gaudin, 1957)	$E_c = \frac{3}{2} R^2$	Interceptional effect; Stokes flow.
(Flint and Howarth, 1971)	$E_c = \frac{V_s}{V_s + U}$	Gravitational effect.
(Reay and Ratcliff, 1973)	$E_c = \frac{V_s}{V_s + U} (1 + R)^2 \sin^2 \varphi_c$	Gravitational effect.

(Anfruns and Kitchener, 1977)	$E_c = \frac{V_s}{V_s + U} (1 + R)^2 + \frac{U}{V_s + U} 2\psi_c$	Combined gravitational and interceptional effects. ψ_c is the stream function ψ calculated at $r = 1 + R$ and $\varphi = \pi / 2$.
(Weber and Paddock, 1983)	$E_c = \frac{V_s}{U} (1 + R)^2 \sin^2 \varphi_c + E_{c,i}$ $E_{c,i} = \frac{3R^2}{2} \left[1 + \frac{3Re/16}{1 + 0.249Re^{0.56}} \right] \dots (*)$ $E_{c,i} = R \left[1 + \frac{2}{1 + (37/Re)^{0.85}} \right] \dots (**)$	Combined gravitational and interceptional effects; intermediate bubble Reynolds number. Eq. (*) for bubbles with a fully immobile surface. Eq. (**) for bubbles with a fully mobile surface.
(Yoon and Luttrell, 1989)	$E_{c,i} = R^2 \left[\frac{3}{2} + \frac{4Re^{0.72}}{15} \right]$	Interceptional effect; intermediate bubble Reynolds number; fully immobile bubble surface.
(Dobby and Finch, 1987)	<p>1) <i>Low particle inertia</i>, $St < 0.1$ $E_{c,0} = E_{c,g} + E_{c,i}$ $E_{c,i}$ is given by Weber and Paddock for immobile surface. $E_{c,g}$ is given by Reay and Ratcliff.</p> $\varphi_c = \begin{cases} 78.1 - 7.37 \log Re & \text{if } 400 > Re > 20 \\ 85.5 - 12.49 \log Re & \text{if } 20 > Re > 1 \\ 85.0 - 2.5 \log Re & \text{if } 1 > Re > 0.1 \end{cases}$ <p>2) <i>Intermediate particle inertia</i>, $St > 0.1$ $E_c = (E_{c,0}) \left[1.627 Re^{0.06} St^{0.54} (V_s / U)^{-0.16} \right]$ $E_{c,0}$ is the low-St efficiency given in 1).</p>	Combined inertial, gravitational and interceptional effects; intermediate bubble Reynolds number; immobile bubble surface; analytical results for low Stokes number, St , and numerical results for intermediate St . $St = \frac{Re \rho}{9 \delta} R^2$ Range of application of the numerical results for intermediate inertia: $300 > Re > 20$; $0.8 > St$; and $0.25 > V_s / U$.
(Schulze, 1989)	$E_c = E_{c,i} + E_{c,g} + E_{c,in} \left[1 - \frac{E_{c,i}}{(1 + R)^2} \right]$ $E_{c,i} = \frac{U}{V_s + U} 2\psi_c$ $E_{c,g} = \frac{V_s}{U} (1 + R)^2 \sin^2 \varphi_c$ $E_{c,in} = \frac{U}{V_s + U} (1 + R)^2 \left(\frac{St}{St + a} \right)^b$ <p>For $R \leq 1 / \xi$:</p> $\psi_c = \frac{4R^2}{2} \left[1 + \frac{3Re/16}{1 + 0.249Re^{0.56}} \right]$	Combined gravitational, inertial and interceptional effects; intermediate bubble Reynolds number; immobile bubble surface; approximate results for both low and intermediate St . Model parameters (a , b and φ_c) are functions of Re . φ_c is given by Dobby and Finch. The surface vorticity is given as $\xi = \frac{3 + \frac{9Re/16}{1 + 0.249Re^{0.56}}}{2 \sin \varphi_c}$
(Dukhin, 1983; Dai et al., 1998)	$E_c = 3R \sin^2 \varphi_c \exp \left\{ -\cos \varphi_c \left[3K''' (\ln R + 1.8) + (8 - 12 \cos \varphi_c + 4 \cos^3 \varphi_c) / (3 \sin^4 \varphi_c) \right] \right\}$	Potential flow and bubbles with a mobile surface. Significant effect of centrifugal force on collision. Valid for ultrafine particles. Expression for the collision

	$\varphi_c = \text{acos}\left(\sqrt{1+\beta^2} - \beta\right)$ $\beta = \frac{2Rf}{3K^m} \text{ and } K^m = \frac{2(\rho - \delta)UR_p^2}{9\mu R_b}$	efficiency is called the Generalized Sutherland Equation (GSE).
(Nguyen and Schulze, 2004)	<p>- Gravitational collision</p> $E_{c,g} = \frac{V_s}{V_s + U}$ <p>- Interceptional collision</p> $E_{c,i} = f(R) \frac{V_s}{V_s + U} \left[X + Y \cos \varphi_{c,i} \right] \sin^2 \varphi_{c,i}$ $\varphi_{c,i} = \text{acos} \left\{ \frac{\sqrt{X^2 + 3Y^2} - X}{3Y} \right\}$ <p>- Inertial collision</p> $E_{c,in} = \frac{(St)^a - b}{(St)^a + c}$ <p>- Simultaneous gravitational and interceptional collision</p> $E_{c,gi} = \frac{f(R)V_s}{V_s + U} \left[X + C + Y \cos \varphi_{c,i} \right] \sin^2 \varphi_{c,gi}$ $\varphi_{c,gi} = \text{acos} \left\{ \frac{\sqrt{(X+C)^2 + 3Y^2} - (X+C)}{3Y} \right\}$ <p>- Overall collision efficiency</p> $E_c = 1 - (1 - E_{c,g})(1 - E_{c,i})(1 - E_{c,in})(1 - E_{c,t})$	<p>Individual and combined inertial, gravitational and interceptional effects; intermediate bubble Reynolds number; immobile and mobile bubble surface; gas hold up; approximate results for both low and intermediate Stokes number, St.</p> <p>Model parameters (a, b, c, X and Y) are functions of Re and gas volume fraction (as well as the bubble surface mobility) – see (Nguyen and Schulze, 2004).</p> <p>For bubbles with an immobile surface, $f(R) = R^2$.</p> <p>For bubbles with a mobile surface, $f(R) = R - R^2$.</p> $C = \frac{V_s}{U} \frac{1}{f(R)}$
(Reay and Ratcliff, 1975; Jiang and Holtham, 1986)	$E_c = m(R)^n$	Empirical or computational results. Model parameters m and n are only available for limited conditions but $n > 1$ for all cases.

Regarding bubble-particle collision interactions in turbulent flows, a stochastic modelling approach must be adopted. The flotation literature on this topic is very limited when compared with the extensive literature dealing with turbulent gas-particle flows and turbulent coagulation of fine particles. Some key features found in the flotation literature are described below:

For turbulent bubble-particle collision interaction, the bubble-particle relative velocity can be decomposed into the time-averaged, $\Delta\bar{\mathbf{V}}$ (deterministic), and fluctuating (stochastic), $\Delta\mathbf{V}'$, components of the relative velocity, yielding

$$\Delta\mathbf{V}(t) = \Delta\bar{\mathbf{V}} + \Delta\mathbf{V}'(t) \quad (25)$$

Substituting Eq. (25) into Eq. (24) we obtain

$$E_e = \frac{\oint \Delta \bar{\mathbf{V}} \cdot d\mathbf{S}_b}{\pi (R_p + R_b)^2 (V_p + U_b)} + \frac{\oint \Delta \mathbf{V}'(t) \cdot d\mathbf{S}_b}{\pi (R_p + R_b)^2 (V_p + U_b)} \quad (26)$$

The collision efficiency now has two terms. Firstly, the first term on the right-hand side of Eq. (26) represents the efficiency due to the time-averaged (mean) interactions (If the time-averaged flow variables are different from zero, the results presented in Table 1 and discussed in the preceding section can be applied). Secondly, the second term is due to the fluctuating relative motion between the bubble and particle (Likewise, the collision frequency β can also have two similar terms). Since $\Delta \mathbf{V}'(t)$ is a random field, the fluctuating collision interaction must be determined by a stochastic approach. Although the fluctuating velocities are random, the mass balance over the bubble surface requires that the overall particle influx and outflux over the bubble surface be equal. The collision frequency due to fluctuating motions, β' , is therefore half the surface area multiplied by the average magnitude of the relative radial velocity, i.e.,

$$\beta' = \oint \Delta \mathbf{V}'(t) \cdot d\mathbf{S}_b = 2\pi (R_p + R_b)^2 \langle |\Delta V_r'| \rangle \quad (27)$$

where $\Delta V_r' = \mathbf{R} \cdot \Delta \mathbf{V}' / R$ is the radial component of the fluctuating relative velocity, \mathbf{R} is the vector of particle centres, and $R = |\mathbf{R}|$. The angle brackets in Eq. (27) describe the statistical average over the colliding sphere which is defined, relative to the bubble, as a sphere of radius $R = R_p + R_b$. The calculation of the averaged velocity in Eq. (27) is central to many theories on turbulent particulate interactions. Principally, the averaged velocity can be determined from the first moment of the velocity, which is derived from the probability distribution function (PDF), $p(\Delta V_r')$, and is given by:

$$\langle |\Delta V_r'| \rangle = \int_{-\infty}^{+\infty} |\Delta V_r'| p(\Delta V_r') d\Delta V_r' \quad (28)$$

where $p(\Delta V_r') d\Delta V_r'$ is the probability of $\Delta V_r'$ taking a value between $\Delta V_r'$ and $\Delta V_r' + d\Delta V_r'$.

The PDF is usually assumed to follow a Gaussian probability distribution

$$p(\Delta V_r') = \frac{1}{\sigma \sqrt{2\pi}} \exp\left(-\frac{\Delta V_r'^2}{2\sigma^2}\right) \quad (29)$$

where $\sigma^2 = \langle \Delta V_r'^2 \rangle$ is the variance (second moment) of $\Delta V_r'$. Inserting Eq. (29) into Eq. (28) and integrating gives

$$\langle |\Delta V_r'| \rangle = \sqrt{\frac{2}{\pi}} \sigma \quad (30)$$

The collision frequency function and efficiency due to turbulence fluctuation are directly proportional to the second moment of the radial fluctuating relative velocity of particles. Inserting Eq. (30) into Eq. (27), the fluctuating collision frequency is given by:

$$\beta' = \sqrt{8\pi} (R_p + R_b)^2 \sigma \quad (31)$$

The calculation of the variance of the fluctuating relative velocity of colliding particles is widely reported in the literature and recently reviewed (Meyer and Deglon, 2011). The available literature is rich but often confusing; especially since the majority of the predictions for the fluctuating collision function for gas-particle flows and particle coagulation in liquids are not physically consistent with the bubble-particle interactions in flotation. The following comments are offered:

1) Both spherical and cylindrical formulations have been used to calculate the turbulent collision frequency function, but models based on the cylindrical formulation are erroneous. The spherical formulation gives rise to Eq. (27) and should be used while the cylindrical formulation uses a cylindrical volume passing through a reference particle per unit time and yields $\beta' = \pi (R_p + R_b)^2 \langle |\Delta V'| \rangle$. The differences between the two formulations include not only the numerical factor of 2 but also the average velocities. In the most cited paper by Saffman and Turner (Saffman and Turner, 1956), both formulations were used, leading to different results which could not be reconciled. These two formulations were shown to produce the same results only under special cases (Wang et al., 1998).

2) There is a similarity of mechanisms governing the deterministic and stochastic collisions. The mechanisms of stochastic collisions include diffusion, shear, accelerative, differential sedimentation and preferential concentration. These mechanisms follow the different forces governing the particle motions as described by Eq. (16). Brownian diffusion is known to govern flotation of nanoparticles (Nguyen et al., 2006), and is not important for flotation processes used in the mineral industry. The shear mechanism governs the particle collision of particles which follow water streamlines and collide due to different positions with the shear flow field. The shear mechanism is similar to the bubble-particle collision by interception in the deterministic models in Table 1. The differential

sedimentation mechanism is analogous to the gravitational collision while the accelerative collision is similar to the inertial models of the deterministic collision.

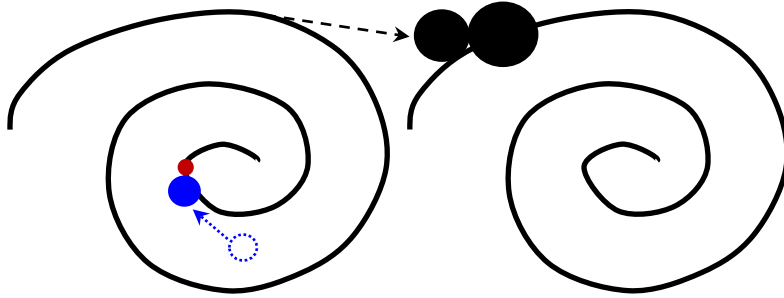


Figure 5. Mechanisms of a particle collision in the turbulent flow field. Small particles (red and blue circles) have velocities correlated with water flow and collide by shear and accelerative correlated mechanisms. Large particles (black circles) have velocities uncorrelated with carrier fluid, can be transferred randomly from eddy to eddy and collide.

3) Unlike the deterministic bubble-particle collisions, the stochastic collisions are significantly controlled by correlation of particle motions in the turbulent flow field (Figure 5). For small particles their fluctuating velocities are correlated or partially correlated with the velocity of carrier fluid. These small particles can collide by either shear flow, difference in accelerations, and gravity. The Saffman and Turner model (Saffman and Turner, 1956) is an excellent description applicable to turbulent collision with a strong correlation. For large particles, their fluctuating velocities are uncorrelated with the velocity of carrier fluid. These large particles are thrown randomly from eddy to eddy and collide. The model of Abrahamson (Abrahamson, 1975) is a good example of the collision of particles with uncorrelated velocities.

Saffman and Turner (Saffman and Turner, 1956) used a simplified version of Eq. (16) without the added-mass force for gas-particle flows and developed a model for the relative velocity variance σ which has three terms due to shear, acceleration and gravity. Their model was corrected using the spherical formulation (Wang et al., 1998), leading to the following prediction:

$$\sigma^2 = \underbrace{\frac{1}{15} R^2 \frac{\varepsilon}{\nu}}_{\text{Shear}} + \underbrace{\left(1 - \frac{\delta}{\rho_p}\right)^2 (\tau_1 - \tau_2)^2 \left\langle \left(\frac{DW}{Dt}\right)^2 \right\rangle}_{\text{Acceleration}} + \underbrace{\frac{\pi}{8} \left(1 - \frac{\delta}{\rho_p}\right)^2 (\tau_1 - \tau_2)^2 g^2}_{\text{Gravity}} + 2 \underbrace{\left(1 - \frac{\delta}{\rho_p}\right)^2 \tau_1 \tau_2 \left\langle \left(\frac{DW}{Dt}\right)^2 \right\rangle \frac{R^2}{\lambda_D^2}}_{\text{Coupling}} \quad (32)$$

where R is the sum of the two particle radii and λ_D is the Taylor microscale of fluid acceleration. The coupling term is absent in the original model and accounts for the combined effect of spatial variation of fluid acceleration and particle inertia. Since air bubbles rise against gravity, and solid particles sink in the direction of gravity, the gravity term applied to the bubble-particle collision should be additive (i.e., $\tau_1 + \tau_2$) because the gravitational forces in Eqs. (16) and (17) are opposite in sign. Moreover, Eq. (32) is strictly valid for fine particles of a size of the smallest eddies and, therefore, has to be modified for flotation to account for the size of air bubbles. A number of modifications and extensions are available as summarised by Meyer and Deglon (Meyer and Deglon, 2011). For flotation, the shear term should also be extended to the inertial subrange using Eq. (7). Also, Eq. (32) has been approximately developed by neglecting the particle acceleration in the motion equation. This approximation can be improved or replaced by the exact solution of the particle motion equation which is described by Eq. (20); where the first term on the right-hand side can give rise to a similar shear term in Eq. (32) and the integral term can be stochastically treated, leading to the other accelerative terms which can contain the following (or similar) integral: $\int_0^\infty e^{-\tau/T} D_L(\tau) d\tau$, where $D_L(\tau)$ is the Lagrangian structure function of fluid flow. The exact approach was briefly described by Panchev (Panchev, 1971), but has since been comprehensively developed for particle turbulent collision by Zaichik et al. in their book (Zaichik et al., 2008).

Large particles exhibit significant inertia when subjected to turbulent fluid flow fluctuation and have velocities uncorrelated with the fluid. Abrahamson (Abrahamson, 1975) assumed the Gaussian probability distribution function for the particle fluctuating velocities in 3D space and calculated the collision rate which can be converted to the collision frequency function as follows:

$$\beta' = 2^{3/2} \pi^{1/2} R^2 \sqrt{(V_1')^2 + (V_2')^2} \quad (33)$$

where R is the sum of the two particle radii. The particle velocity variances in Eq. (33) are obtained using the solution of Eq. (16) and an exponential form for the Lagrangian velocity correlation. Alternatively, the experimental correlations obtained by Liepe and Möckel (Liepe and Moeckel, 1976) can be used. These correlations are as follows:

$$\sqrt{(V_i')^2} = 0.685 \frac{\varepsilon^{4/9} R_i^{7/9}}{\nu^{1/3}} \left(\frac{\rho_p - \delta}{\delta} \right)^{2/3} \quad \text{for } i = 1 \text{ and } 2 \quad (34)$$

Equations (33) and (34) are commonly used to model flotation systems (Schubert, 1999; Pyke et al., 2003; Kostoglou et al., 2006), where Eq. (34) was established based on the balance between the

inertial subrange acceleration (Table 2) and Allen's fluid drag on particles. This balance is appropriate for air bubbles in flotation, with a constant value 0.83 instead of 0.685 (Nguyen and Schulze, 2004), but cannot be used for solid particles in flotation. The appropriate balance for the particles is between dissipative subrange acceleration and Stokes' drag. Therefore, for bubble-particle interactions in flotation then (Nguyen and Schulze, 2004):

$$\sqrt{(U_b')^2} = 0.83 \frac{\varepsilon^{4/9} R_b^{7/9}}{\nu^{1/3}} \left(\frac{\delta - \rho_b}{\delta} \right)^{2/3} \quad (35)$$

$$\sqrt{(V_p')^2} = \frac{2R_p^3}{135} \frac{\varepsilon}{\nu^2} \frac{\rho_p - \delta}{\delta} \quad (36)$$

When body forces, such as the gravitational forces which drive the particle settling and bubble rising in flotation are considered, the Abrahamson solution can be converted to the collision frequency function as follows (Nguyen and Schulze, 2004):

$$\beta' = R^2 (V_p + U_b) \chi \left[\frac{\sqrt{V_p'^2 + U_b'^2}}{V_s + U_b} \right] \quad (37)$$

where function χ is defined by $\chi(x) = 2^{3/2} \pi^{1/2} x \exp\left\{-\frac{1}{2x^2}\right\} + \pi(1+x^2) \operatorname{erf}\left\{\frac{1}{\sqrt{2}x}\right\}$. Since $\chi(0) = 1$ as in the case of no turbulence (the bar variables are zero), the collision is expected under a constant force field of gravity. If gravity is ignored ($V_s + U_b \rightarrow 0$), Eq. (37) reduces to Eq. (33).

Finally, the proposed models need experimental validation.

5. EFFECT OF TURBULENCE ON DETACHMENT

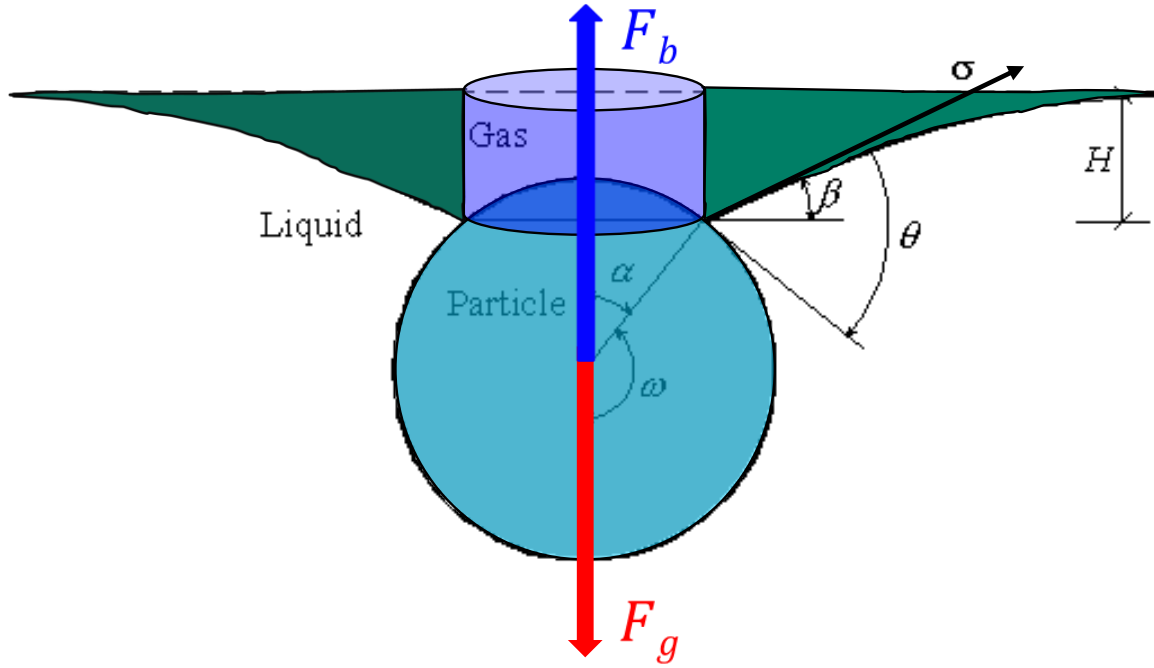


Figure 6. Force balance on a spherical particle attached to the air-water surface shows the validity of the Archimedes Principle: $\mathbf{F}_b = \mathbf{F}_g$.

Quantifying the stability of bubble-particle aggregates in flotation aims to determine if the adhesion on the attached particle is strong for supporting the particle to avoid detaching from the bubble surface by the disruptive forces in flotation cells. The force analysis on the attached particle concludes that the Archimedes Principle still holds for equilibrium of the particle attachment to the air-water interface: The weight of liquid displaced by air (of volume enclosed by the deformed air-water interface, air-solid interface, and the initial plane) is balanced by the particle weight, i.e.,

$$F_b = F_g \quad (38)$$

where buoyancy consists of the liquid weights of volumes above the deformed air-water interface and the cylinder above the three-phase contact area less the spherical cap. These three volumes are highlighted in green, purple and dark blue in Figure 6. The liquid weight of the first volume is equal to the vertical component of capillary force (Nguyen and Schulze, 2004). It gives:

$$F_b = 2\pi R_p \sigma \sin \alpha \sin \beta + \pi (R_p \sin \alpha)^2 H \delta g - \frac{(2 - 3 \cos \alpha + \cos^3 \alpha) \pi R_p^3}{3} \delta g \quad (39)$$

The particle weight in Eq. (38) is constant, whilst the buoyancy supporting the stability of the particle is a function of the polar contact position. Due to the geometry constraint, $\theta = \alpha + \beta$, the

capillary force exhibits a maximum at $\alpha = \beta = \theta / 2$. Buoyancy also has a maximum, called the tenacity of particle attachment, which can be described as follows:

$$T = \max \{F_b\} = \pi R_p \sigma (1 - \cos \theta) \left\{ 1 + 0.016 \sqrt{Bo} + O(Bo) \right\} \quad (40)$$

where $Bo = (R_p / L)^2$ is the Bond number and $L = \sqrt{\sigma / (\delta g)}$ is the capillary length, which is about 2.7 mm for the air-water surface at room temperature. The cut-off terms of Eq. (40) are of the order of the Bond number, which is satisfactorily met by the particle size in flotation ($Bo \gg 1$).

The effect of the bubble size on the tenacity of particle attachment has been investigated by Nguyen (Nguyen, 2003), whom showed that the tenacity of a bubble-particle couplet is described as follows:

$$T = \pi R_p \sigma \left(\sqrt{1 + 2A \cos \theta + A^2} - \cos \theta - A \right) + O(Bo^{3/2}) \quad (41)$$

where $A = Bo(1 - R_b / L)$.

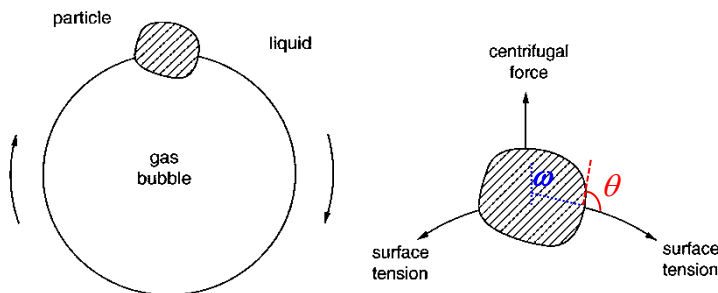


Figure 7. A bubble-particle couplet rotating in a turbulent eddy (left) and the forces acting on the particle (right) (Jameson et al., 2007).

Knowing the tenacity of particle attachment then the efficiency of bubble-particle stability and detachment can be computed and then used to predict the maximum size of floatable particle (Pyke et al., 2003; Nguyen and Schulze, 2004; Jameson et al., 2007; Goel and Jameson, 2012). In addition to the particle weight, turbulence has a significant role in disrupting the bubble-particle aggregates. In particular, in a mechanical flotation cell the region surrounding by the impeller and stator is highly turbulent and it is here that most of the energy is imparted to the flotation slurry to produce air bubbles and promote the bubble-particle interactions. Turbulence in the impeller-stator region influences not only the collision but also the detachment. Typically, the results are described

in terms of either “machine acceleration”, b_m , or the mean energy dissipation rate. Schulze (Schulze, 1983) considered that air bubbles in the impeller region behaved as if they were at the centre of a vortex, so they rotated with the vortex as shown in Figure 7. The rotational velocity was found using isotropic turbulence theory. Any particle on the surface of the bubble would experience a centrifugal force tending to move the particle away from the bubble. For the machine acceleration case, Schulze (1982) used the acceleration of turbulence in the inertial subrange described by Eq. (15), which gives

$$b_m = 1.9 \frac{\varepsilon^{2/3}}{R_b^{1/3}} \quad (42)$$

The machine acceleration is then added to the right-hand side of Eq. (38) which can be balanced by the tenacity of particle attachment to determine the upper limit of floatable particle size. For a particle much smaller than the relevant bubble it can be shown that the maximum particle size that remains attached to a bubble is as follows:

$$R_{p\max} = \sqrt{\frac{3\sigma(1 - \cos \theta)}{4\rho_p (g + b_m)}} \quad (43)$$

For larger particles, the maximum particle size can be obtained by solving the following nonlinear equation: $\pi R_p \sigma (\sqrt{1 + 2A \cos \theta + A^2} - \cos \theta - A) = \frac{4\pi R_p^3 \rho_p}{3} (g + b_m)$. Table 3 shows the results of the calculation and comparison with flotation experimental data.

Table 3. Dependence of the maximum size of floatable sylvinite particles on the acceleration of turbulent eddies (Nguyen, 2002).

b_m/g	$R_{p\max}$ (μm)	
	Eq. (43)	Experimental
4.45	708	700
8.75	529	480
12.10	457	430

The calculation of the machine acceleration described by Eq. (42) requires the bubble size, which is usually a variable in flotation. It can be estimated based on the effect of microturbulence on the stability of air bubbles, i.e., the bubble size in the impeller region is also controlled by pressure fluctuation of microturbulence (Nguyen and Schulze, 2004). The pressure tends to break-

up the bubble, which is resisted by the surface tension force. Equation (12) for the pressure fluctuation of the inertial subrange is usually used. Balancing the two forces gives the following prediction for the bubble size (Jameson et al., 2007):

$$R_{b\max} = 3.27 \left(\frac{\sigma^{3/5}}{\varepsilon_i^{2/5} \delta^{3/5}} \right) \quad (44)$$

where ε_i is the power per unit mass based on the mass of liquid in the volume swept by the impeller. The machine acceleration appropriate to the maximum bubble size is obtained by substituting Eq. (44) into Eq. (42), giving:

$$b_m^* = 1.28 \varepsilon_i^{4/5} \delta^{1/5} / \sigma^{1/5} \quad (45)$$

Inserting Eq. (45) into Eq. (43), with $b_m \ll g$, yields the following approximate equation for the maximum floatable particle size:

$$R_{p\max} = 0.77 \left\{ \frac{\sigma^{6/5} (1 - \cos \theta)}{\rho_p \varepsilon_i^{4/5} \delta^{1/5}} \right\}^{1/2} \quad (46)$$

Equation (46) can be tested using the following conditions (Jameson et al., 2007):

- 1) Mechanical flotation cell with power input of 3 kW/m³,
- 2) Swept volume of the impeller is one-tenth of the volume of the liquid in the cell, giving a power consumption in the impeller region of 30 kW/m³,
- 3) Chalcopyrite particles of density 4200 kg/m³, in a pulp of density 1200 kg/m³, and
- 4) Surface tension of 60 mN/m, and the contact angle of 60 degrees.

Equation (46) gives a maximum floatable particle size of 500 μm , which is within the range of expectations.

Knowing the maximum floatable particle size, the efficiency, E_s , of the bubble-particle aggregate stability in the turbulent field can be predicted as follows:

$$E_s = 1 - \exp \left\{ 1 - \left(\frac{R_{p\max}}{R_p} \right)^2 \right\} = 1 - \exp \left\{ 1 - \frac{0.59 \sigma^{6/5} (1 - \cos \theta)}{R_p^2 \rho_p \varepsilon_i^{4/5} \delta^{1/5}} \right\} \quad (47)$$

Limits of the current theoretical developments

The presented theoretical developments for bubble-particle stability and detachment are derived when the turbulent tensile stresses are dominant. Shear stresses outlined by the transverse acceleration described by Eq. (14) can also be significant. If the turbulent shear stresses or the vibration of bubble-particle aggregates rising to the pulp-froth interface are the dominant forces causing the particle detachment, the theories have to be modified, as shown in the literature (Nguyen and Schulze, 2004). Significantly, the current theories are based on constant, single-valued contact angle. Practically, the contact angle is multi-valued and varies from the receding (minimum) to advancing (maximum) values. The contact variation known as the contact angle hysteresis is due to the fact that the particle surface is almost always rough and chemically heterogeneous; and therefore the resistance to the triple contact line relaxation during the advancing event is different from that during the receding event. Since detachment is an advancing event, the advancing contact angle can be applied to the current theory if the contact angle is narrowly distributed and contact angle hysteresis is small. Recent work (Feng and Nguyen, 2016) showed that the pinning of the contact line at the sharp edge, known as the Gibbs inequality condition (GIC), can play a significant role in controlling the stability and detachment of floating spheres. In this study, the spheres were truncated with different angles and the force of pushing the truncated spheres from the interface into water was measured. Both the experimental and theoretical results confirmed the critical effect of GIC on stability and detachment of floating spheres as shown in Figure 8. For small angles of truncation, GIC did not affect the sphere detachment and hence the classical theories on the floatability of spheres are valid. For large truncated angles, GIC determined the tenacity of the particle-meniscus contact and the stability and detachment of floating spheres, and the classical theories were invalid. The detaching force between an air bubble and a cubical particle has also shown to be influenced by the shape edge of the particle (Gautam and Jameson, 2012).

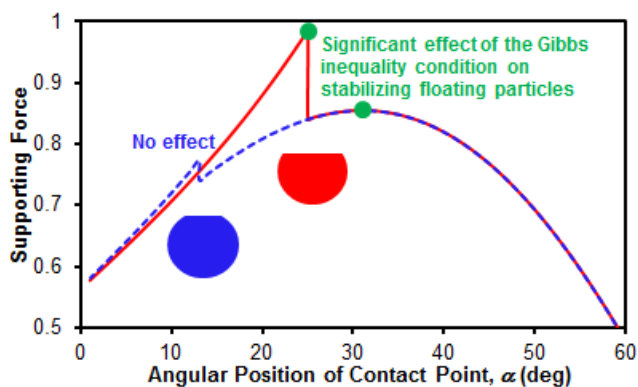


Figure 8. Effect of pinning of the contact line at the sharp edge, known as the Gibbs inequality condition, on stability and detachment of floating spheres (Feng and Nguyen, 2016). The vertical axis shows the supporting force of buoyancy (depicted in Figure 6) normalised by dividing by

$2\pi\sigma R_p$. During the detachment by advancing of triple contact line from the spherical surface to the planar surface of truncation, the advancing contact angle changes from θ to $\theta + \alpha_0 + \pi/2$, where α_0 is the half-filling angle of truncation, leading to a shape increase in the supporting force. For a large angle of truncation, the increase in the supporting force exceeds the tenacity of attachment predicted at $\alpha = \theta/2$ (approximately) by the classical theory which otherwise fails to explain the stability of the floating sphere in this case.

CONCLUSIONS

In this paper the literature on the quantification of the effect of microturbulence on bubble-particle interaction in flotation has been reviewed. While the theory on microturbulence of water flow is well developed, the stochastic description of particle and bubble motions in the turbulent flow field in the mechanical flotation cells is limited. The deterministic modelling of bubble-particle collision interaction is well developed and can be used to approximate the interaction by the mean (time-averaged) turbulent flow. The effect of microturbulence on bubble-particle collision is less quantified despite the literature on particle-particle turbulent collision in gas-particle flow and coagulation is very rich. The application of the particle-particle collision models for flotation is not straightforward because of the different properties of air bubbles, namely, large size and rise velocity as opposite to settling of particles. Further analysis of the particle-particle collision models reveals similar mechanisms governing bubble-particle collision in flotation because the governing forces are similar. The cylindrical formulation for modelling turbulent collision is enormous and should not be used. Abrahamson's turbulent collision frequency functions modified to account for the variance of fluctuating velocities for air bubbles and solid particles would be a good approximation for flotation. No quantitative models of the bubble-particle turbulent collision efficiency relevant for flotation are available. Modelling bubble-particle turbulent detachment has been based on balancing the tenacity of buoyancy forces and centrifugal force using the mean machine acceleration estimated from microturbulence theory. There still exist a number of deficiencies in modelling bubble-particle turbulent detachment. The majority of studies only consider the particle turbulent acceleration in the centrifugal direction but ignore the transverse acceleration of particles, which is due to turbulent shear flow. Contact angle required in quantifying the detachment is not constant as considered in the current theories, but are multi-valued and can invalidate the theories if there is a significant contact angle hysteresis. The latest experiments based on the Gibbs inequality condition show that multi-valued contact angle can significant affect stability and detachment of floating particles. Further research is required for quantifying the effect of microturbulence on bubble-particle interaction in flotation.

ACKNOWLEDGEMENTS

This research is supported under Australian Research Council's Projects funding schemes (project number DP150100395).

REFERENCES

- Abrahamson, J., 1975. Collision rates of small particles in a vigorously turbulent fluid. *Chemical Engineering Science*, 30(11): 1371-1379.
- Anfruns, J.F. and Kitchener, J.A., 1977. Rate of capture of small particles in flotation. *Trans. Inst. Min. Metall. (Sect. C)*, 86: 9-15.
- Batchelor, G.K., 1982. *The theory of homogenous turbulence*. Cambridge University Press, Cambridge, 197 pp.
- Dai, Z., Dukhin, S., Fornasiero, D. and Ralston, J., 1998. The inertial hydrodynamic interaction of particles and rising bubbles with mobile surfaces. *J. Colloid Interface Sci.*, 197(2): 275-292.
- Dai, Z., Fornasiero, D. and Ralston, J., 2000. Particle-bubble collision models - a review. *Adv. Colloid Interface Sci.*, 85(2-3): 231-256.
- Dobby, G.S. and Finch, J.A., 1986. A model of particle sliding time for flotation size bubbles. *J. Colloid Interface Sci.*, 109(2): 493-98.
- Dobby, G.S. and Finch, J.A., 1987. Particle size dependence in flotation derived from a fundamental model of the capture process. *Int. J. Miner. Process.*, 21(3-4): 241-60.
- Dukhin, S.S., 1983. Critical value of the Stokes number and the Sutherland formula. *Kolloidn. Zh.*, 45(2): 207-18.
- Feng, D. and Nguyen, A.V., 2016. How does the Gibbs inequality condition affect the stability and detachment of floating spheres from the free surface of water? *Langmuir*, 32: DOI: 10.1021/acs.langmuir.5b04098
- Flint, L.R. and Howarth, W.J., 1971. Collision efficiency of small particles with spherical air bubbles. *Chem. Eng. Sci.*, 26(8): 1155-68.
- Gaudin, A.M., 1957. *Flotation*. McGraw-Hill, New York.
- Gautam, A. and Jameson, G.J., 2012. The capillary force between a bubble and a cubical particle. *Miner. Eng.*, 36-38: 291-299.
- Goel, S. and Jameson, G.J., 2012. Detachment of particles from bubbles in an agitated vessel. *Miner. Eng.*, 36-38: 324-330.
- Guerra, E.A. and Schubert, H., 1997. Effects of some important parameters on fine particle entrainment during flotation in mechanical cells, *Proc. XX Int. Miner. Process. Congr., Aachen, Germany*, pp. 153-165.
- Jameson, G.J., Nguyen, A.V. and Ata, S., 2007. The flotation of fine and coarse particles. In: M.C. Fuerstenau, G.J. Jameson and R.-H. Yoon (Editors), *Froth Flotation: A Century of Innovation*. SME, Denver, CO, USA, pp. 329-351.
- Jameson, G.J. and S. Nam, M.M.Y., 1977. Physical factors affecting recovery rates in flotation. *Minerals Science and Engineering*, 9(No. 3. July 1977): 103.
- Jiang, Z.W. and Holtham, P.N., 1986. Theoretical model of collision between particles and bubbles in flotation. *Institute of Mining and Metallurgy*, 95: C187-C194.
- King, R.P., 2001. *Modeling and Simulation of Mineral Processing Systems*. Elsevier.
- Kolmogorov, A.N., 1941. Local structure of turbulence in noncompressible fluid with very high Reynolds number. *Doklady Acad. Sci. USSR*, 30: 168-181.
- Kostoglou, M., Karapantsios, T.D. and Matis, K.A., 2006. Modeling local flotation frequency in a turbulent flow field. *Advances in colloid and interface science*, 122(1): 79-91.

- Kruis, F. and Kusters, K., 1997. The collision rate of particles in turbulent flow. *Chemical Engineering Communications*, 158(1): 201-230.
- Liepe, F. and Moeckel, H.O., 1976. Studies of the combination of substances in liquid phase. Part 6: The influence of the turbulence on the mass transfer of suspended particles. *Chem. Tech. (Leipzig)*, 28(4): 205-9.
- Lynch, A.J., Harbort, G.J. and Nelson, M.G., 2010. *History of Flotation*. The Australasian Institute of Mining and Metallurgy, Burwood, Vic, Australia, 348 pp.
- Meyer, C.J. and Deglon, D.A., 2011. Particle collision modelling - A review. *Miner. Eng.*, 24: 719-730.
- Nguyen, A.V., 2002. New method and equations for determining attachment tenacity and particle size limit in flotation. *Inter. J. Min. Process.*, 68: 167-182.
- Nguyen, A.V., 2003. New method and equations for determining attachment tenacity and particle size limit in flotation. *International journal of mineral processing*, 68(1): 167-182.
- Nguyen, A.V., 2011. Particle-bubble interaction in flotation. In: R. Miller and L. Liggieri (Editors), *Bubble and drop interfaces*. Progress in Colloid and Interface Science. Brill, Leiden, The Netherland.
- Nguyen, A.V., George, P. and Jameson, G.J., 2006. Demonstration of a minimum in the recovery of nanoparticles by flotation: theory and experiment. *Chem. Eng. Sci.*, 61: 2494-2509.
- Nguyen, A.V. and Schulze, H.J., 2004. *Colloidal science of flotation*. Marcel Dekker, New York, 840 pp.
- Panchev, S., 1971. *Random functions and turbulence*. Pergamon Press, Oxford.
- Phan, C.M., Nguyen, A.V., Miller, J.D., Evans, G.M. and Jameson, G.J., 2003. Investigations of bubble-particle interactions. *International Journal of Mineral Processing*, 72(1): 239-254.
- Pyke, B., Fornasiero, D. and Ralston, J., 2003. Bubble particle heterocoagulation under turbulent conditions. *Journal of colloid and interface science*, 265(1): 141-151.
- Ralston, J., Dukhin, S.S. and Mishchuk, N.A., 1999. Inertial hydrodynamic particle-bubble interaction in flotation. *Int. J. Miner. Process.*, 56(1-4): 207-256.
- Reay, D. and Ratcliff, G.A., 1973. Removal of fine particles from water by dispersed air flotation. Effects of bubble size and particle size on collection efficiency. *Can. J. Chem. Eng.*, 51: 178-85.
- Reay, D. and Ratcliff, G.A., 1975. Experimental testing of the hydrodynamic collision model of fine particle flotation. *Can. J. Chem. Eng.*, 53(5): 481-6.
- Saffman, P. and Turner, J., 1956. On the collision of drops in turbulent clouds. *Journal of Fluid Mechanics*, 1(01): 16-30.
- Schubert, H., 1999. On the turbulence-controlled microprocesses in flotation machines. *International journal of mineral processing*, 56(1): 257-276.
- Schubert, H. and Bischofberger, C., 1978. On the hydrodynamics of flotation machines. *Int. J. Miner. Process.*, 5(2): 131-42.
- Schubert, H. and Bischofberger, C., 1998. On the microprocesses air dispersion and particle-bubble attachment in flotation machines as well as consequences for the scale-up of macroprocesses. *Int. J. Miner. Process.*, 52(4): 245-259.
- Schubert, H., Heidenreich, E., Liepe, F. and Neesse, T., 1990. *Mechanische Verfahrenstechnik*. Deutscher Verlag für Grundstoffindustrie, Leipzig, 407 pp.
- Schulze, H.J., 1982. Dimensionless number and approximate calculation of the upper particle size of floatability in flotation machines. *Int. J. Miner. Process.*, 9(4): 321-8.
- Schulze, H.J., 1983. *Physicochemical elementary processes in flotation*. Elsevier Science Publishers, 1983: 348.
- Schulze, H.J., 1989. Hydrodynamics of bubble-mineral particle collisions. *Miner. Process. Extract. Met. Rev.*, 5: 43-76.
- Sutherland, K., 1948. The physical chemistry of flotation XI. Kinetics of the flotation process. *J. Phys. Chem.*, 52: 394-425.
- Wang, L.-P., Wexler, A.S. and Zhou, Y., 1998. Statistical mechanical descriptions of turbulent coagulation. *Physics of Fluids*, 10: 2647-2651.

- Weber, M.E. and Paddock, D., 1983. Interceptional and gravitational collision efficiencies for single collectors at intermediate Reynolds numbers. *J. Colloid Interface Sci.*, 94(2): 328-35.
- Williams, J. and Crane, R., 1983. Particle collision rate in turbulent flow. *International Journal of Multiphase Flow*, 9(4): 421-435.
- Yoon, R.H. and Luttrell, G.H., 1989. The effect of bubble size on fine particle flotation. *Miner. Proc. Extract. Met. Rev.*, 5: 101-122.
- Zaichik, L.I., Alipchenkov, V.M. and Sinaiski, E.G., 2008. *Particles in turbulent flows*. Wiley-VCH Verlag GmbH, Weinheim, Germany.